



A posteriori error estimation for the fractional step theta discretization of the incompressible Navier–Stokes equations

Dominik Meidner^a, Thomas Richter^{b,*}

^a Chair of Optimal Control, Technische Universität München, Boltzmannstraße 3, 85748 Garching b. Munich, Germany

^b Institute of Applied Mathematics, University of Heidelberg, INF 294, 69120 Heidelberg, Germany

Available online 3 December 2014

Highlights

- A goal-oriented a posteriori error estimator for time-discretization with the Fractional-Step Theta Method is introduced.
- We introduce a Petrov–Galerkin formulation, that is – up to a quadrature error – equivalent to the Fractional-Step Theta time-stepping scheme.
- This new error estimator is applied to nonstationary incompressible flow problems.

Abstract

In this work, we derive a goal-oriented a posteriori error estimator for the error due to time discretization. As time discretization scheme we consider the fractional step theta method, that consists of three subsequent steps of the one-step theta method. In every sub-step, the full incompressible system has to be solved (in contrast to time integrators of operator splitting type). The resulting fractional step theta method combines various desirable properties like second order accuracy, strong A-stability and very little numerical dissipation.

The derived error estimator is based on a mathematical trick: we define an intermediate time-discretization scheme based on a Petrov–Galerkin formulation. This method is up to a numerical quadrature error equivalent to the theta time stepping scheme. The error estimator is assembled as one weighted residual term given by the Dual Weighted Residual method measuring the error between real solution and solution to the Petrov–Galerkin formulation (that at no time has to be calculated) and one additional residual estimating the discrepancy between actual time stepping scheme used for simulation and the intermediate Petrov–Galerkin formulation.

© 2014 Elsevier B.V. All rights reserved.

Keywords: Incompressible Navier–Stokes; Fractional step theta; Time stepping; Adaptivity; Error estimation

1. Introduction

In this work, we develop a technique for goal-oriented error estimation and time step adaption for the incompressible Navier–Stokes equations, discretized with the fractional step theta method. This time stepping method, introduced

* Corresponding author.

E-mail addresses: meidner@ma.tum.de (D. Meidner), thomas.richter@iwr.uni-heidelberg.de (T. Richter).

by Glowinski et al. [1,2] is one of the most attractive time discretization schemes for incompressible flows, as it combines several attributes like strong A-stability, very little numerical dissipation and second order accuracy. To avoid confusion, we note that we are not applying the fractional step theta method as an operator splitting scheme. One step $t_{m-1} \rightarrow t_m$ of the fractional step theta method is combined from three substeps of the one-step theta scheme, here formulated for the time-discretization of a simple initial value problem $u'(t) = f(t, u(t))$:

$$u_k^m - u_k^{m-1} = \theta kf(t^m, u_k^m) + (1 - \theta)kf(t^{m-1}, u_k^{m-1}).$$

Applied to the Navier–Stokes equations, one step of the fractional step theta method requires three sub-steps with the full saddle point system.

For such a traditional finite difference approximation, a posteriori error control and time step adaption are usually based on estimation of the truncation error. In [3], the authors presented a new technique of error estimation for the theta and fractional theta method for parabolic problems. This error estimator is based on the following idea: The discrete solution u_k^m for $m = 1, 2, \dots, M$ is calculated with the theta time stepping method. As we cannot directly estimate the error $u(t_m) - u_k^m$ between the numerical solution and the real solution, we introduce an intermediate problem based on a Galerkin formulation of a variational problem of the Navier–Stokes equations. This Galerkin solution is referred to as u_k^G . Now, the discretization error can be split by the triangle inequality

$$|u(t_m) - u_k^m| \leq |u(t_m) - u_k^G(t_m)| + |u_k^G(t_m) - u_k^m|,$$

and two separate errors must be estimated. Estimating the first contribution is a standard task for Galerkin methods and can be accomplished by residual estimation. The second error contribution turns out to be given by a numerical quadrature error, that describes the difference between the time stepping method and the Galerkin method. Finally, we note out, that the Galerkin scheme is only used as mathematical construct. At no time it will be necessary to compute or approximate its solution u_k^G .

For error estimation, the goal-oriented approach going back to Becker and Rannacher [4,5] is employed. In particular considering problems in fluid-dynamics, one is very often interested in technical quantities like drag coefficients. By goal-oriented error estimation we can estimate the error and optimize the mesh specifically with respect to such functionals.

In this article, we generalize the error estimation technique described in [3] for parabolic problems to the incompressible Navier–Stokes equations by a suitable treatment of the divergence-free condition.

The following two sections will give the mathematical setting and background of the error estimator. The focus of Section 2 will be a Galerkin formulation for the incompressible Navier–Stokes equations similar to the theta method. Then, in Section 3 we derive the a posteriori error estimator based on this Galerkin formulation. In Section 4, we summarize the error estimator and describe the adaptive procedure as a computational approach usable in applications. In Section 5, we present numerical examples, demonstrating the accuracy of the error estimator and the efficiency of locally refined time discretizations.

2. Time-Galerkin discretizations of the Navier–Stokes equations

Let $\Omega \subset \mathbb{R}^d$ be a two ($d = 2$) or three ($d = 3$) dimensional domain with smooth or convex polygonal boundary and $I = (0, T)$ be a time interval. By $L^2(\Omega)$ we denote the Lebesgue space of square integrable functions and by $H_0^1(\Omega; \Gamma)$ the Sobolev space of square integrable functions with first weak derivatives in $L^2(\Omega)$ and trace zero on (parts of) the boundary $\Gamma \subset \partial\Omega$, with $H_0^1(\Omega) := H_0^1(\Omega; \partial\Omega)$. Further, we introduce the Hilbert spaces X^v and X^p defined as

$$X^v = \{v \mid v \in L^2(I, V) \text{ and } \partial_t v \in L^2(I, V^*)\}, \quad X^p = L^2(I, H),$$

with $V = H_0^1(\Omega; \Gamma)^d$, $H = L^2(\Omega)$, and the dual space V^* of V . We denote the pair of the spaces X^v and X^p by $\mathcal{X} = X^v \times X^p$. The inner product of $L^2(I, H)$ and the duality pairing between $L^2(I, V)$ and $L^2(I, V^*)$ are defined as

$$(p, q)_I := \int_I (p(t), q(t))_H dt \quad \text{and} \quad \langle u, v \rangle_I := \int_I \langle u(t), v(t) \rangle_{V \times V^*} dt.$$

The extension of $(\cdot, \cdot)_I$ to function from $L^2(I, H^d)$ is straightforward.

Problem 1 (Navier–Stokes Equations). Let $\mathbf{v}^0 \in V$ and $\mathbf{f} \in L^2(I, H^d)$. Find $(\mathbf{v}, p) \in \mathcal{X}$, such that $\mathbf{v}(0) = \mathbf{v}^0$ and

$$\langle \partial_t \mathbf{v}, \boldsymbol{\varphi} \rangle_I + \int_I \{a(\mathbf{v}, \boldsymbol{\varphi}) - b(p, \boldsymbol{\varphi}) + b(\boldsymbol{\xi}, \mathbf{v})\} dt = (\mathbf{f}, \boldsymbol{\varphi})_I \quad \forall (\boldsymbol{\varphi}, \boldsymbol{\xi}) \in \mathcal{X}, \tag{1}$$

where $a(\mathbf{v}, \boldsymbol{\varphi}) = \nu(\nabla \mathbf{v}, \nabla \boldsymbol{\varphi}) + (\mathbf{v} \cdot \nabla \mathbf{v}, \boldsymbol{\varphi})$ and $b(p, \boldsymbol{\varphi}) = (p, \nabla \cdot \boldsymbol{\varphi})$.

In the sequel, we will write (1) compressed as

$$A(\mathbf{u})(\boldsymbol{\Phi}) = F(\boldsymbol{\Phi}) \quad \forall \boldsymbol{\Phi} \in \mathcal{X}$$

with $\mathbf{u} = (\mathbf{v}, p) \in \mathcal{X}$, $\boldsymbol{\Phi} = (\boldsymbol{\varphi}, \boldsymbol{\xi}) \in \mathcal{X}$, and

$$\begin{aligned} A(\mathbf{u})(\boldsymbol{\Phi}) &= (\mathbf{v}(0), \boldsymbol{\varphi}(0)) + \langle \partial_t \mathbf{v}, \boldsymbol{\varphi} \rangle_I + \int_I \{a(\mathbf{v}, \boldsymbol{\varphi}) - b(p, \boldsymbol{\varphi}) + b(\boldsymbol{\xi}, \mathbf{v})\} dt, \\ F(\boldsymbol{\Phi}) &= (\mathbf{f}, \boldsymbol{\varphi})_I + (\mathbf{v}^0, \boldsymbol{\varphi}(0)). \end{aligned} \tag{2}$$

2.1. Time stepping formulation

For a temporal approximation of the Navier–Stokes equations we introduce a subdivision of the time-interval I as

$$0 = t_0 < t_1 < \dots < t_M = T, \quad k_m := t_m - t_{m-1}, \quad k := \max_{m=1, \dots, M} k_m.$$

The theta time stepping scheme as basis for the fractional step theta method is then given as a finite difference approximation of Problem 1:

Problem 2 (Theta Time-stepping Scheme). Let $\theta = (\theta_m)_{m=1}^M \in [0, 1]^M$ and $\mathbf{v}_{k,0}^\theta = \mathbf{v}^0$. Find $\mathbf{v}_k^\theta = (\mathbf{v}_{k,m}^\theta)_{m=1}^M \in V^M$ and $p_k^\theta = (p_{k,m}^\theta)_{m=1}^M \in H^M$ by iterating for $m = 1, 2, \dots, M$:

$$\begin{aligned} (\mathbf{v}_{k,m}^\theta - \mathbf{v}_{k,m-1}^\theta, \boldsymbol{\varphi}) + \theta_m k_m a(\mathbf{v}_{k,m}^\theta, \boldsymbol{\varphi}) + (1 - \theta_m) k_m a(\mathbf{v}_{k,m-1}^\theta, \boldsymbol{\varphi}) - k_m b(p_{k,m}^\theta, \boldsymbol{\varphi}) + k_m b(\boldsymbol{\xi}, \mathbf{v}_{k,m}^\theta) \\ = \theta_m k_m (\mathbf{f}(t_m), \boldsymbol{\varphi}) + (1 - \theta_m) k_m (\mathbf{f}(t_{m-1}), \boldsymbol{\varphi}) \quad \forall (\boldsymbol{\varphi}, \boldsymbol{\xi}) \in V \times H. \end{aligned} \tag{3}$$

The pressure is considered as a Lagrange multiplier for realizing the divergence condition at time t_m , it hence fully appears on the implicit side. The fractional step theta method is based on this one step theta scheme by combining three substeps

$$t_{m-1} \rightarrow t_{m-1+\alpha} \rightarrow t_{m-\alpha} \rightarrow t_m,$$

using time step sizes αk_m , $(1 - 2\alpha)k_m$, and αk_m . It is shown, e.g., in [1], that the resulting scheme is second order accurate, if we choose $\alpha = 1 - \sqrt{1/2} \approx 0.293$. Each of the three substeps is a theta step, using the three values θ , $1 - \theta$ and again θ . For every $\theta \in (1/2, 1]$ strong A-stability of the combined scheme is given, see [1,2].

2.2. Galerkin in time formulation

In [3], we have derived a Galerkin formulation for the theta time-stepping scheme applied to nonlinear parabolic problems. A direct application to the incompressible Navier–Stokes equations in the same spirit is hindered by the incompressibility constraint.

First, using the temporal grid given above, we consider a partitioning of the time interval $\bar{I} = [0, T]$ as

$$\bar{I} = \{0\} \cup I_1 \cup I_2 \cup \dots \cup I_M$$

with subintervals $I_m = (t_{m-1}, t_m]$ of size k_m . On this subdivision, we define the trial space for velocities and pressure as the piece-wise linears and piece-wise constants by

$$\begin{aligned} X_k^v &= \{\mathbf{v}_k \in C(\bar{I}, V) \mid \mathbf{v}_k|_{I_m} \in \mathcal{P}_1(I_m, V), \quad m = 1, 2, \dots, M\} \\ X_k^p &= \{p_k \in L^2(I; H) \mid p_k|_{I_m} \in \mathcal{P}_0(I_m, H), \quad m = 1, 2, \dots, M\}. \end{aligned}$$

The pair of these discrete trial spaces is denoted by $\mathcal{X}_k^v = \mathbf{X}_k^v \times X_k^p$. For $\mathbf{v}_k \in \mathbf{X}_k^v$, we set $\mathbf{v}_{k,m} = \mathbf{v}_k(t_m)$ and for $p_k \in X_k^p$, we define $p_{k,m} = p_k|_{I_m}$.

As test-space for the momentum equations, we choose

$$\mathbf{X}_{k,\theta}^v = \{\boldsymbol{\varphi}_k \in L^2(I, \mathbf{V}) \mid \boldsymbol{\varphi}_k|_{I_m} \in \mathcal{P}^\theta(I_m, \mathbf{V}), m = 1, 2, \dots, M, \boldsymbol{\varphi}_k(0) \in \mathbf{V}\},$$

where by $\mathcal{P}^\theta(I_m, \mathbf{V})$ we denote the function space

$$\mathcal{P}^\theta(I_m, \mathbf{V}) = \{\bar{\Phi}_m \bar{\boldsymbol{\varphi}}_{k,m} \mid \bar{\boldsymbol{\varphi}}_{k,m} \in \mathbf{V}\}$$

with the theta-weighted function $\bar{\Phi}_m : I_m \rightarrow \mathbb{R}$ defined as

$$\bar{\Phi}_m(t) = 1 + 6\left(\theta_m - \frac{1}{2}\right) \frac{2t - t_{m-1} - t_m}{k}.$$

For the incompressibility constraint, we take the space of piece-wise constants X_k^p as test space. The pair of test-spaces is then denoted by $\mathcal{X}_k^\theta = \mathbf{X}_{k,\theta}^v \times X_k^p$.

Restriction of [Problem 1](#) to these discrete trial and test spaces yields the following formulation:

Problem 3 (Galerkin in Time Formulation). Let $\theta = (\theta_m)_{m=1}^M \in [0, 1]^M$ and $\mathbf{v}_{k,0} = \mathbf{v}^0$. Find $\mathbf{u}_k = (\mathbf{v}_k, p_k) \in \mathcal{X}_k$ such that

$$A(\mathbf{u}_k)(\bar{\boldsymbol{\Phi}}_k) = F(\bar{\boldsymbol{\Phi}}_k) \quad \forall \bar{\boldsymbol{\Phi}}_k \in \mathcal{X}_k^\theta,$$

where A and F are given by (2).

Calculating the concrete forms of A and F for the discrete ansatz and test spaces yields

$$\begin{aligned} A(\mathbf{u}_k)(\bar{\boldsymbol{\Phi}}_k) &= (\mathbf{v}_{k,0}, \boldsymbol{\varphi}_{k,0}) + \sum_{m=1}^M \left\{ (\mathbf{v}_{k,m} - \mathbf{v}_{k,m-1}, \bar{\boldsymbol{\varphi}}_{k,m}) \right. \\ &\quad + k_m \theta_m (\nabla \mathbf{v}_{k,m}, \nabla \bar{\boldsymbol{\varphi}}_{k,m}) + k_m (1 - \theta_m) (\nabla \mathbf{v}_{k,m-1}, \nabla \bar{\boldsymbol{\varphi}}_{k,m}) \\ &\quad - k_m (p_{k,m}, \nabla \cdot \bar{\boldsymbol{\varphi}}_{k,m}) + \int_{I_m} (\mathbf{v}_k \cdot \nabla \mathbf{v}_k, \boldsymbol{\varphi}_k) dt \\ &\quad \left. + \frac{k_m}{2} (\nabla \cdot \mathbf{v}_{k,m-1}, \xi_{k,m}) + \frac{k_m}{2} (\nabla \cdot \mathbf{v}_{k,m}, \xi_{k,m}) \right\}, \\ F(\bar{\boldsymbol{\Phi}}_k) &= \sum_{m=1}^M \int_{I_m} (\mathbf{f}, \boldsymbol{\varphi}_k) dt + (\mathbf{v}^0, \boldsymbol{\varphi}_{k,0}). \end{aligned} \tag{4}$$

Hence, the discrete variational formulation (4) of [Problem 3](#) shows two differences compared to the theta time stepping scheme (3) of [Problem 2](#):

1. The nonlinearity $\mathbf{v} \cdot \nabla \mathbf{v}$ and the right hand side \mathbf{f} are in (4) not approximated as in (3). This can be overcome by applying numerical quadrature, the key concept in [3].
2. In contrast to (3), the incompressibility constraint is not fully taken implicitly in (4). Instead, this scheme gives rise to the relation

$$\|\nabla \cdot \mathbf{v}_{k,m}\| = \|\nabla \cdot \mathbf{v}_{k,m-1}\|$$

which is not desirable in terms of stability. It will be the main contribution of this paper to extend the theory from [3] to the incompressible Navier–Stokes equations while capturing the divergence condition completely implicitly.

3. Goal-oriented error estimation

A posteriori error estimation and adaptive time mesh discretization will be based on the dual weighted residual method (DWR) by Becker and Rannacher [4,5] that has already been applied to different Galerkin formulations of the incompressible Navier–Stokes equations, see, e.g., [6,7].

In [3], the authors derived an a posteriori error estimator for the theta and fractional step theta time-stepping scheme applied to parabolic problems. To extend this approach, we start the derivation of an a posteriori error estimate by introducing the following equivalent formulation for the finite difference theta scheme of **Problem 2**: Find $\mathbf{u}_k^\theta \in \mathcal{X}_k$ such that

$$A_\theta(\mathbf{u}_k^\theta)(\Phi_k) = F_\theta(\Phi_k) \quad \forall \Phi_k \in \mathcal{X}_k^\theta \tag{5}$$

with

$$A_\theta(\mathbf{u}_k^\theta)(\Phi_k) = (\mathbf{v}_{k,0}^\theta, \varphi_{k,0}) + \sum_{m=1}^M \{ (\mathbf{v}_{k,m}^\theta - \mathbf{v}_{k,m-1}^\theta, \bar{\varphi}_k^m) + \theta_m k_m a(\mathbf{v}_{k,m}^\theta, \bar{\varphi}_{k,m}) + (1 - \theta_m) k_m a(\mathbf{v}_{k,m-1}^\theta, \bar{\varphi}_{k,m}) - k_m b(p_{k,m}^\theta, \bar{\varphi}_{k,m}) + k_m b(\xi_{k,m}, \mathbf{v}_{k,m}^\theta) \}$$

and

$$F_\theta(\Phi_k) = \sum_{m=1}^M \{ \theta_m k_m (f(t_m), \bar{\varphi}_{k,m}) + (1 - \theta_m) k_m (f(t_{m-1}), \bar{\varphi}_{k,m}) \} + (\mathbf{v}^0, \varphi_{k,0}).$$

For a differentiable error functional $J: \mathcal{X} \rightarrow \mathbb{R}$ given by

$$J(\mathbf{u}) = \int_I j_1(\mathbf{u}(t)) dt + j_2(\mathbf{u}(T)),$$

where $j_1, j_2: \mathbf{V} \times H \rightarrow \mathbb{R}$ we define three Lagrange functionals on $\mathcal{X} \times \mathcal{X}$ as well as on $\mathcal{X}_k \times \mathcal{X}_k^\theta$ by

$$\begin{aligned} L(\mathbf{u})(\mathbf{z}) &= J(\mathbf{u}) + F(\mathbf{z}) - A(\mathbf{u})(\mathbf{z}), \\ L(\mathbf{u}_k)(\mathbf{z}_k) &= J(\mathbf{u}_k) + F(\mathbf{z}_k) - A(\mathbf{u}_k)(\mathbf{z}_k), \\ L_\theta(\mathbf{u}_k^\theta)(\mathbf{z}_k^\theta) &= J(\mathbf{u}_k^\theta) + F_\theta(\mathbf{z}_k^\theta) - A_\theta(\mathbf{u}_k^\theta)(\mathbf{z}_k^\theta), \end{aligned}$$

where by $\mathbf{z} = (\mathbf{w}, q) \in \mathcal{X}$, $\mathbf{z}_k = (\mathbf{w}_k, q_k) \in \mathcal{X}_k$, and $\mathbf{z}_k^\theta = (\mathbf{w}_k^\theta, q_k^\theta) \in \mathcal{X}_k^\theta$ we denote adjoint variables solving

$$A'(\mathbf{u})(\Phi, \mathbf{z}) = J'(\mathbf{u})(\Phi) \quad \forall \Phi \in \mathcal{X} \tag{6a}$$

$$A'(\mathbf{u}_k)(\Phi_k, \mathbf{z}_k) = J'(\mathbf{u}_k)(\Phi_k) \quad \forall \Phi_k \in \mathcal{X}_k \tag{6b}$$

$$A'_\theta(\mathbf{u}_k^\theta)(\Phi_k, \mathbf{z}_k^\theta) = J'(\mathbf{u}_k^\theta)(\Phi_k) \quad \forall \Phi_k \in \mathcal{X}_k. \tag{6c}$$

Remark 1. The derivatives A' and A'_θ are given by

$$A'(\mathbf{u})(\Phi, \mathbf{z}) = (\varphi(0), \mathbf{w}(0)) + \langle \partial_t \varphi, \mathbf{w} \rangle_I + \int_I \{ a'(\mathbf{v})(\varphi, \mathbf{w}) - b(\xi, \mathbf{w}) + b(q, \varphi) \} dt$$

and

$$\begin{aligned} A'_\theta(\mathbf{u}_k^\theta)(\Phi_k, \mathbf{z}_k^\theta) &= (\varphi_{k,0}, \mathbf{w}_{k,0}^\theta) + \sum_{m=1}^M \{ (\varphi_{k,m} - \varphi_{k,m-1}, \bar{\mathbf{w}}_{k,m}^\theta) + \theta_m k_m a'(\mathbf{v}_{k,m}^\theta)(\varphi_{k,m}, \bar{\mathbf{w}}_{k,m}^\theta) \\ &\quad + (1 - \theta_m) k_m a'(\mathbf{v}_{k,m-1}^\theta)(\varphi_{k,m-1}, \bar{\mathbf{w}}_{k,m}^\theta) - k_m b(\xi_{k,m}, \bar{\mathbf{w}}_{k,m}^\theta) + k_m b(q_{k,m}^\theta, \varphi_{k,m}) \}. \end{aligned} \tag{7}$$

In the following, we will analyze the difference between the theta method as time-stepping scheme and as a Galerkin formulation, i.e., between the **Problems 2** and **3**. As mentioned before, this difference stems from the approximation of the divergence condition and from the approximation of the nonlinearity by numerical quadrature. To capture the latter effect, [3, Lemma 3.2] shows for the test space weight Φ_m and all $v \in W^{2,1}(I_m, \mathbb{R})$ that

$$\int_{I_m} v(t) \Phi_m(t) dt = \theta_m k_m v(t_m) + (1 - \theta_m) k_m v(t_{m-1}) + \mathcal{R}_m(v) \tag{8a}$$

holds with a remainder bounded by

$$|\mathcal{R}_m(v)| \leq k_m^2 \|\partial_t^2 v\|_{L^1(I, \mathbb{R})}. \tag{8b}$$

Application of this quadrature formula to the Navier–Stokes equations and their adjoint and treating the error due to the approximation of the divergence condition yields:

Lemma 1 (Quadrature Error). *Let $\mathbf{f} \in H^2(I, H^d)$. Then, for any $\mathbf{u}_k = (\mathbf{v}_k, p_k) \in \mathcal{X}_k$ and any test function $\Phi_k = (\boldsymbol{\varphi}_k, \xi_k) \in \mathcal{X}_k^\theta$, it holds*

$$F(\boldsymbol{\psi}_k) - A(\mathbf{u}_k)(\Phi_k) = F_\theta(\Phi_k) - A_\theta(\mathbf{u}_k)(\boldsymbol{\psi}_k) + \mathcal{R}^p(\mathbf{u}_k, \Phi_k).$$

Furthermore, for any $\mathbf{u}_k, \Phi_k \in \mathcal{X}_k$ and $\mathbf{z}_k \in \mathcal{X}_k^\theta$ it holds

$$J'(\mathbf{u}_k)(\Phi_k) - A'(\mathbf{u}_k)(\Phi_k, \mathbf{z}_k) = J'(\mathbf{u}_k)(\Phi_k) - A_{\theta'}(\mathbf{u}_k)(\Phi_k, \mathbf{z}_k) + \mathcal{R}^d(\mathbf{u}_k, \Phi_k, \mathbf{z}_k).$$

The remainder terms can be estimated as

$$|\mathcal{R}^p(\mathbf{u}_k, \Phi_k)| \leq Ck^2 \left(\sum_{m=1}^M k_m \|\bar{\boldsymbol{\varphi}}_{k,m}\|^2 \right)^{\frac{1}{2}} \{ \|\partial_t \mathbf{v}_k \cdot \nabla \partial_t \mathbf{v}_k\|_I + \|\partial_t^2 \mathbf{f}\|_I \} + Ck \|\xi_k\|_I \|\nabla \cdot \partial_t \mathbf{v}_k\|_I$$

and

$$|\mathcal{R}^d(\mathbf{u}_k, \Phi_k, \mathbf{z}_k)| \leq Ck^2 \left(\sum_{m=1}^M k_m \|\bar{\mathbf{w}}_{k,m}\|^2 \right)^{\frac{1}{2}} \{ \|\partial_t \mathbf{v}_k \cdot \partial_t \nabla \boldsymbol{\varphi}_k\|_I + \|\partial_t \boldsymbol{\varphi}_k \cdot \partial_t \nabla \mathbf{v}_k\|_I \} + Ck \|q_k\|_I \|\nabla \cdot \partial_t \boldsymbol{\varphi}_k\|_I.$$

Proof. To estimate the remainder terms \mathcal{R}^p and \mathcal{R}^d only nonlinear terms, the right-hand sides, and the divergence conditions in primal and dual equations have to be considered, cf. the proof of Lemma 3.3 in [3].

- (i) First, we consider the right-hand side $(\mathbf{f}, \boldsymbol{\varphi}_k)_I$ and the convection term $(\mathbf{v}_k \cdot \nabla \mathbf{v}_k, \boldsymbol{\varphi}_k)_I$ in the primal equations. Application of (8) gives for the integration error of the primal equation

$$\begin{aligned} |\mathcal{R}_1^p| &= \left| \sum_{m=1}^M \left\{ \int_{I_m} (\mathbf{f}, \boldsymbol{\varphi}_k) \, dt - \theta_m k_m (\mathbf{f}(t_m), \bar{\boldsymbol{\varphi}}_{k,m}) - (1 - \theta_m) k_m (\mathbf{f}(t_{m-1}), \bar{\boldsymbol{\varphi}}_{k,m}) \right\} \right| \\ &\leq \sum_{m=1}^M k_m^2 \|(\partial_t^2 \mathbf{f}, \bar{\boldsymbol{\varphi}}_{k,m})\|_{L^1(I_m, \mathbb{R})} \leq Ck^2 \left(\sum_{m=1}^M k_m \|\bar{\boldsymbol{\varphi}}_{k,m}\|^2 \right)^{\frac{1}{2}} \|\partial_t^2 \mathbf{f}\|_I, \end{aligned}$$

and using that \mathbf{v}_k is piecewise linear in time yields

$$\begin{aligned} |\mathcal{R}_2^p| &= \left| \sum_{m=1}^M \left\{ \int_{I_m} (\mathbf{v}_k \cdot \nabla \mathbf{v}_k, \boldsymbol{\varphi}_k) - \theta_m k_m (\mathbf{v}_{k,m} \cdot \nabla \mathbf{v}_{k,m}, \bar{\boldsymbol{\varphi}}_{k,m}) \right. \right. \\ &\quad \left. \left. - (1 - \theta_m) k_m (\mathbf{v}_{k,m-1} \cdot \nabla \mathbf{v}_{k,m-1}, \bar{\boldsymbol{\varphi}}_{k,m-1}) \right\} \right| \\ &\leq \sum_{m=1}^M k_m^2 \|(\partial_t^2 [\mathbf{v}_k \cdot \nabla \mathbf{v}_k], \bar{\boldsymbol{\varphi}}_{k,m})\|_{L^1(I_m, \mathbb{R})} \\ &= \sum_{m=1}^M k_m^2 2 \|(\partial_t \mathbf{v}_k \cdot \nabla \partial_t \mathbf{v}_k, \bar{\boldsymbol{\varphi}}_{k,m})\|_{L^1(I_m, \mathbb{R})} \\ &\leq Ck^2 \left(\sum_{m=1}^M k_m \|\bar{\boldsymbol{\varphi}}_{k,m}\|^2 \right)^{\frac{1}{2}} \|\partial_t \mathbf{v}_k \cdot \nabla \partial_t \mathbf{v}_k\|_I. \end{aligned}$$

- (ii) The adjoint residual shows a remainder due to integration only for the derivative of the nonlinearity, $(\mathbf{v}_k \cdot \nabla \boldsymbol{\varphi}_k + \boldsymbol{\varphi}_k \cdot \nabla \mathbf{v}_k, \mathbf{w}_k)$, that can be estimated as in the first case by

$$\begin{aligned} |\mathcal{R}_1^d| &\leq \sum_{m=1}^M k_m^2 \|(\partial_t^2 [\mathbf{v}_k \cdot \nabla \boldsymbol{\varphi}_k + \boldsymbol{\varphi}_k \cdot \nabla \mathbf{v}_k], \bar{\mathbf{w}}_{k,m})\|_{L^1(I_m, \mathbb{R})} \\ &\leq Ck^2 \left(\sum_{m=1}^M k_m \|\bar{\mathbf{w}}_{k,m}\|^2 \right)^{\frac{1}{2}} \{ \|\partial_t \mathbf{v}_k \cdot \partial_t \nabla \boldsymbol{\varphi}_k\|_I + \|\partial_t \boldsymbol{\varphi}_k \cdot \partial_t \nabla \mathbf{v}_k\|_I \}. \end{aligned}$$

(iii) Finally, both remainders carry error terms that stem from the approximation of the divergence condition. Here we cannot apply Lemma 3.2 of [3]. Instead, we directly estimate for piece-wise constant $\xi_k \in X_k^p$ the error between the exact divergence condition and its approximation by the box rule:

$$\begin{aligned} \frac{k_m}{2}(\nabla \cdot \mathbf{v}_{k,m-1}, \xi_{k,m}) + \frac{k_m}{2}(\nabla \cdot \mathbf{v}_{k,m}, \xi_{k,m}) &= \int_{I_m} (\nabla \cdot \mathbf{v}_k, \xi_k) \, dt \\ &= k_m(\nabla \cdot \mathbf{v}_{k,m}, \xi_{k,m}) - \frac{k_m}{2} \int_{I_m} (\nabla \cdot \partial_t \mathbf{v}_k, \xi_k) \, dt. \end{aligned}$$

Hence, we get for this error contribution

$$\begin{aligned} |\mathcal{R}^{\text{div}}(\mathbf{v}_k, \xi_k)| &= \left| \frac{k_m}{2}(\nabla \cdot \mathbf{v}_{k,m-1}, \xi_{k,m}) + \frac{k_m}{2}(\nabla \cdot \mathbf{v}_{k,m}, \xi_{k,m}) - k_m(\nabla \cdot \mathbf{v}_k^m, \xi_k^m) \right| \\ &\leq Ck|(\nabla \cdot \partial_t \mathbf{v}_k, \xi_k)_I| \leq Ck\|\xi_k\|_I \|\nabla \cdot \partial_t \mathbf{v}_k\|_I. \end{aligned}$$

The complete primal and dual remainder terms are finally given by

$$\begin{aligned} \mathcal{R}^p(\mathbf{u}_k, \Phi_k) &= \mathcal{R}_1^p + \mathcal{R}_2^p + \mathcal{R}^{\text{div}}(\mathbf{v}_k, \xi_k), \\ \mathcal{R}^d(\mathbf{u}_k, \Phi_k, \mathbf{z}_k) &= \mathcal{R}_1^d + \mathcal{R}^{\text{div}}(\varphi_k, q_k). \quad \square \end{aligned}$$

With help of these estimates on the quadrature error that measures the difference between theta scheme (Problem 2) and Galerkin formulation (Problem 3), we can formulate the main result, an a posteriori error estimator for the functional error:

Theorem 1. Let $\mathbf{u} \in \mathcal{X}$ be the solution to Problem 1, $\mathbf{u}_k^\theta \in \mathcal{X}_k$ the solution to Problem 2 and $\mathbf{z} \in \mathcal{X}$ as well as $\mathbf{z}_k^\theta \in \mathcal{X}_k^\theta$ be the adjoint solutions given by (6a) and (6c). For the functional error due to time discretization it holds

$$J(\mathbf{u}) - J(\mathbf{u}_k^\theta) = \rho(\mathbf{u}_k^\theta)(\mathbf{z}_k^\theta) + \frac{1}{2} \{ \rho(\mathbf{u}_k^\theta)(\mathbf{z} - \Pi_k^\theta \mathbf{z}) + \rho^*(\mathbf{u}_k^\theta, \mathbf{z}_k^\theta)(\mathbf{u} - \Pi_k \mathbf{u}) \} + \mathcal{R}_k,$$

with the primal and dual residuals

$$\rho(\mathbf{u})(\psi) := F(\psi) - A(\mathbf{u})(\psi), \quad \rho^*(\mathbf{u}, \mathbf{z})(\psi) := J'(\mathbf{u})(\psi) - A'(\mathbf{u})(\psi, \mathbf{z})$$

and a remainder \mathcal{R}_k given by

$$\mathcal{R}_k = \mathcal{R}^{(3)} + \mathcal{R}^p(\mathbf{u}_k, \pi_k^\theta \mathbf{z} - \mathbf{z}_k^\theta) + \mathcal{R}^d(\mathbf{u}_k, i_k \mathbf{u} - \mathbf{u}_k^\theta, \mathbf{z}_k).$$

Here, $\Pi_k: \mathcal{X} \rightarrow \mathcal{X}_k$ and $\Pi_k^\theta: \mathcal{X} \rightarrow \mathcal{X}_k^\theta$ are defined by means of the nodal interpolant $i_k: \mathbf{X}^v \rightarrow \mathbf{X}_k^v$ and the L^2 projections $\pi_k: X^p \rightarrow X_k^p$ and $\pi_k^\theta: \mathbf{X}^v \rightarrow \mathbf{X}_{k,\theta}^v$ as $\Pi_k = (i_k, \pi_k)$ and $\Pi_k^\theta = (\pi_k^\theta, \pi_k)$. The remainder $\mathcal{R}^{(3)}$ is the standard remainder of the dual weighted residual estimator, see Section 3.1. The remainders \mathcal{R}^p and \mathcal{R}^d are given in Lemma 1.

Proof. Since \mathbf{u} solves (1) and \mathbf{u}_k^θ is a solution of (5), it holds by the definition of L and L_θ that

$$\begin{aligned} J(\mathbf{u}) - J(\mathbf{u}_k^\theta) &= L(\mathbf{u}, \mathbf{z}) - L_\theta(\mathbf{u}_k^\theta, \mathbf{z}_k^\theta) \\ &= \underbrace{L(\mathbf{u}, \mathbf{z}) - L(\mathbf{u}_k^\theta, \mathbf{z}_k^\theta)}_{(I)} + \underbrace{L(\mathbf{u}_k^\theta, \mathbf{z}_k^\theta) - L_\theta(\mathbf{u}_k^\theta, \mathbf{z}_k^\theta)}_{(II)}. \end{aligned}$$

The second term (II) is measuring the difference between Galerkin formulation and theta scheme. It holds

$$(II) = \underbrace{J(\mathbf{u}_k^\theta) - J(\mathbf{u}_k^\theta)}_{=0} + F(\mathbf{z}_k^\theta) - A(\mathbf{u}_k^\theta)(\mathbf{z}_k^\theta) + \underbrace{F_\theta(\mathbf{z}_k^\theta) - A_\theta(\mathbf{u}_k^\theta)(\mathbf{z}_k^\theta)}_{=0},$$

and we derive a first computable part of the error estimator. Part (I) can be estimated following the usual DWR theory as

$$L(\mathbf{u}, \mathbf{z}) - L(\mathbf{u}_k^\theta, \mathbf{z}_k^\theta) = \frac{1}{2} L'(\mathbf{u}_k^\theta, \mathbf{z}_k^\theta)(\mathbf{u} - \mathbf{u}_k^\theta, \mathbf{z} - \mathbf{z}_k^\theta) + \mathcal{R}^{(3)}(\mathbf{u} - \mathbf{u}_k^\theta, \mathbf{z} - \mathbf{z}_k^\theta).$$

The remainder is of third order in the errors of primal and adjoint problem, see, e.g., [5,3]. As we cannot apply Galerkin orthogonality, insertion of interpolants yields

$$\begin{aligned} L'(\mathbf{u}_k^\theta, \mathbf{z}_k^\theta)(\mathbf{u} - \mathbf{u}_k^\theta, \mathbf{z} - \mathbf{z}_k^\theta) \\ = L'(\mathbf{u}_k^\theta, \mathbf{z}_k^\theta)(\mathbf{u} - \Pi_k \mathbf{u}, \mathbf{z} - \Pi_k^\theta \mathbf{z}) + L'(\mathbf{u}_k^\theta, \mathbf{z}_k^\theta) \underbrace{(\Pi_k \mathbf{u} - \mathbf{u}_k^\theta)}_{=: \eta_k^u} \underbrace{(\Pi_k^\theta \mathbf{z} - \mathbf{z}_k^\theta)}_{=: \eta_k^z}. \end{aligned}$$

Here, the first part exactly establishes the two remaining residual parts of the estimator. It remains to show, that the last term is of higher order, such that it does not significantly influence the estimator. Using Lemma 1, it holds

$$\begin{aligned} L'(\mathbf{u}_k^\theta, \mathbf{z}_k^\theta)(\eta_k^u, \eta_k^z) &= \{F(\eta_k^z) - A(\mathbf{u}_k^\theta)(\eta_k^z)\} + \{J'(\mathbf{u}_k^\theta)(\eta_k^u) - A'(\mathbf{u}_k^\theta)(\eta_k^u, \mathbf{z}_k^\theta)\} \\ &= \{F_\theta(\eta_k^z) - A_\theta(\mathbf{u}_k^\theta)(\eta_k^z)\} + \{J'(\mathbf{u}_k^\theta)(\eta_k^u) - A_\theta'(\mathbf{u}_k^\theta)(\eta_k^u, \mathbf{z}_k^\theta)\} \\ &\quad + \mathcal{R}^p(\mathbf{u}_k, \eta_k^z) + \mathcal{R}^d(\mathbf{u}_k, \eta_k^u, \mathbf{z}_k) \\ &= \mathcal{R}^p(\mathbf{u}_k^\theta, \eta_k^z) + \mathcal{R}^d(\mathbf{u}_k^\theta, \eta_k^u, \mathbf{z}_k), \end{aligned}$$

such that only remainders by numerical quadrature are left. \square

Remark 2. As exact primal and adjoint solution enter the interpolation weights of the estimator, we cannot strictly speak of an a posteriori error estimator. In Section 3.3 we discuss computational techniques for approximating these weights by known quantities only.

3.1. Discussion of the remainders

Altogether, the estimator derived in Theorem 1 carries three remainders,

$$\mathcal{R}_k = \mathcal{R}^{(3)} + \mathcal{R}^p(\mathbf{u}_k, \Pi_k^\theta \mathbf{z} - \mathbf{z}_k^\theta) + \mathcal{R}^d(\mathbf{u}_k, \Pi_k \mathbf{u} - \mathbf{u}_k^\theta, \mathbf{z}_k).$$

The first one is the standard remainder of the DWR method, that comes from the application of the trapezoidal rule. For the Navier–Stokes equations, this remainder behaves as

$$|\mathcal{R}^{(3)}| \leq |((\mathbf{v} - \mathbf{v}_k) \cdot \nabla(\mathbf{v} - \mathbf{v}_k), (\mathbf{z} - \mathbf{z}_k))_I| + |J'''(\mathbf{u}_k)(\mathbf{u} - \mathbf{u}_k, \mathbf{u} - \mathbf{u}_k, \mathbf{u} - \mathbf{u}_k)|.$$

Both parts – being of third order in the error – are small provided the error $\mathbf{u} - \mathbf{u}_k$ is small.

The other two remainders come from the discrepancy between the time-stepping and Galerkin version of the theta scheme. By use of Lemma 1 and proceeding as in [3, Remark 4.2] employing the stability of the projections operators i_k and π_k^θ , we get for \mathcal{R}^p

$$\begin{aligned} |\mathcal{R}^p(\mathbf{u}_k, \pi_k^\theta \mathbf{z} - \mathbf{z}_k^\theta)| &\leq Ck^2 \left(\sum_{m=1}^M k_m \|\overline{(\pi_k^\theta \mathbf{w} - \mathbf{w}_k^\theta)_m}\|^2 \right)^{\frac{1}{2}} \{ \|\partial_t \mathbf{v}_k \cdot \nabla \partial_t \mathbf{v}_k\|_I \\ &\quad + \|\partial_t^2 \mathbf{f}\|_I \} + Ck \|\pi_k^\theta q - q_k^\theta\|_I \|\nabla \cdot \partial_t \mathbf{v}_k\|_I \\ &\leq Ck^2 \|\mathbf{w} - \mathbf{w}_k^\theta\|_I \{ \|\partial_t \mathbf{v}_k \cdot \nabla \partial_t \mathbf{v}_k\|_I + \|\partial_t^2 \mathbf{f}\|_I \} + Ck \|q - q_k^\theta\|_I \|\nabla \cdot \partial_t \mathbf{v}_k\|_I, \end{aligned}$$

where the first term is of third order in k (since the approximation error $\mathbf{w} - \mathbf{w}_k^\theta$ of the adjoint theta scheme will be of a least first order k , see [8] for a discussion on adjoint solutions to the Crank–Nicolson scheme). The second term is a purely spatial error with $\|\nabla \cdot \partial_t \mathbf{v}_k\| = O(h^{r_v})$, where $r_v > 0$ is the polynomial degree of the velocity space. Hence, we end up with a mixed remainder of $O(k^2 h^{r_v})$. For \mathcal{R}^d , by a similar estimate also the order $O(k^3 + k^2 h^{r_v})$ is obtained.

3.2. Adjoint solution

The error estimator is based on both the discrete and continuous adjoint solutions $\mathbf{z}_k^\theta \in \mathcal{X}_k^\theta$ of (6c) and $\mathbf{z} \in \mathcal{X}$ of (6a). We will see in the following section, that a computational method can be based on \mathbf{z}_k^θ only. Comparing (7), we can reorder the sums of the variational formulation to establish a time-stepping scheme $\mathbf{z}_{k,m+1}^\theta \rightarrow \mathbf{z}_{k,m}^\theta$ backwards

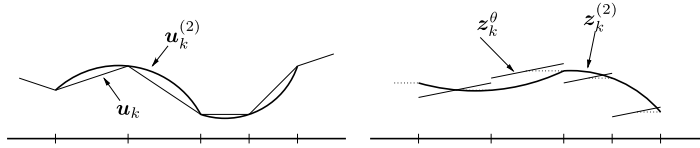


Fig. 1. Piece-wise quadratic reconstructions $u_k^{(2)}$ and $z_k^{\theta(2)}$ of the discrete solutions u_k and z_k .

in time:

$$\begin{aligned}
 A'_\theta(u_k^\theta)(\Phi_k, z_k^\theta) &= (\varphi_{k,M}, \bar{w}_{k,M}^\theta) + \theta_M k_M a'(v_{k,M}^\theta)(\varphi_{k,M}, \bar{w}_{k,M}^\theta) + k_M b(q_{k,M}^\theta, \varphi_{k,M}) - k_M b(\xi_{k,M}, \bar{w}_{k,M}^\theta) \\
 &+ \sum_{m=1}^{M-1} \{ -(\bar{w}_{k,m+1}^\theta - \bar{w}_{k,m}^\theta, \varphi_{k,m}) + \theta_m k_m a'(v_{k,m}^\theta)(\varphi_{k,m}, \bar{w}_{k,m}^\theta) \\
 &+ (1 - \theta_{m+1}) k_{m+1} a'(v_{k,m}^\theta)(\varphi_{k,m}, \bar{w}_{k,m+1}^\theta) + k_m b(q_{k,m}^\theta, \varphi_{k,m}) - k_m b(\xi_{k,m}, \bar{w}_{k,m}^\theta) \} \\
 &- (\bar{w}_{k,1}^\theta - \bar{w}_{k,0}^\theta, \varphi_{k,0}) + (1 - \theta_1) k_1 a'(v_{k,0}^\theta)(\varphi_{k,0}, \bar{w}_{k,1}^\theta).
 \end{aligned}$$

Note, that for computing the adjoint solution, we must distinguish the first and the last from the intermediate steps.

In the case of linear functionals, the corresponding right hand side is given by

$$\begin{aligned}
 \int_I j_1(\Phi_k) dt &= \sum_{m=1}^M \frac{k_m}{2} (j_1(\Phi_{k,m-1}) + j_1(\Phi_{k,m})) \\
 &= \frac{k_1}{2} j_1(\Phi_{k,0}) + \sum_{m=1}^{M-1} \frac{k_m + k_{m+1}}{2} j_1(\Phi_{k,m}) + \frac{k_M}{2} j_1(\Phi_{k,M}).
 \end{aligned}$$

The right hand side for general functionals will depend on the specific choice of $J(\cdot)$. Further, general nonlinear functionals require higher order integration of $\int_I j_1(\Phi) dt$, e.g., by a two-point Gauß formula.

3.3. Approximation of the weights

One of the critical points for applying the dual weighted residual method is the evaluation of the interpolation weights $u - i_k u$ and $z - \pi_k^\theta z$. Basically, two approaches are possible: First, one can numerically compute approximations \hat{u}_k^θ and \hat{z}_k^θ on finer time grids and approximate $u - i_k u \approx \hat{u}_k^\theta - u_k^\theta$ and $z - \pi_k^\theta z \approx \hat{z}_k^\theta - z_k^\theta$. This approach is not feasible due to the large computational effort. Second, relying on super-convergence results – that however cannot be strictly proved for equations like the incompressible Navier–Stokes equations – one can reconstruct higher order approximations $u_k^{(2)}$ of u_k^θ and $z_k^{\theta(2)}$ of z_k^θ and approximate the interpolation errors as

$$u - i_k u \approx u_k^{(2)} - u_k^\theta, \quad z - \pi_k^\theta z \approx z_k^{\theta(2)} - z_k^\theta.$$

Here, we choose this second approach, that is computationally very efficient and usually results in good approximations. Even though less accuracy is required for the adjoint solution, we assemble $u_k^{(2)}$ and $z_k^{\theta(2)}$ piece-wise quadratic reconstructions of the discrete solutions. Fig. 1 shows this reconstruction process and [3] gives some analysis on the super-approximation properties of this reconstruction. For this reconstruction to give a higher order, we must assume that M is even and that two subsequent intervals each have the same step length, e.g.,

$$\underbrace{|t_{m+1} - t_m|}_{=k_{m+1}} = \underbrace{|t_{m+2} - t_{m+1}|}_{=k_{m+2}}, \quad m = 0, 2, 4, \dots, M - 2.$$

This is easily established by using patched meshes in time, i.e. every time-mesh can be considered as one global refinement of an adaptive mesh.

3.4. Application to the fractional step theta method

As the fractional step theta method is constructed by three substeps of the theta time-stepping method, and as $\theta = (\theta_m)_{m=1}^M$ was chosen piece-wise, the error estimator stated in Theorem 1 is directly applicable. For practical

purposes we only need to modify the reconstruction process for evaluation of the weights $\mathbf{u} - i_k \mathbf{u}$ and $\mathbf{z} - \pi_k^\theta \mathbf{z}$. The intermediate steps $t_{m \pm \alpha}$ of the fractional step theta method are not necessarily good approximations to the solution. Hence, these steps are omitted in the reconstruction procedure. Instead, we construct a piece-wise quadratic reconstruction using the macro-time steps, only. Again, consult [3] for details.

4. An adaptive feed-back algorithm for solving the incompressible Navier–Stokes equations

In the following, we will present an adaptive algorithm based on the error estimator introduced in the previous sections. We give details on every step of solution, adjoint solution, error estimation and time-mesh adaptation. Most of the description goes analogously for the one step and fractional step theta method.

First, let $\{t_m \mid m = 0, 1, \dots, M\}$ be an initial subdivision of $\bar{I} = [0, T]$ into discrete time steps with step size $k_m := t_m - t_{m-1}$. Further let $\theta = (\theta_m)_{m=1}^M \in [0, 1]^M$ be a selection of θ -parameters. If, we consider the classical fractional step theta method, the choices of t_m and θ_m must be such, that M is a multiple of 3 and that it holds with $\alpha = 1 - \sqrt{1/2}$ and $\bar{\theta} \in (\frac{1}{2}, 1]$ for $j = 1, 2, \dots, \frac{M}{3}$ that

$$\begin{aligned} t_{3j+1} - t_{3j} &= \alpha(t_{3j+3} - t_{3j}) & \theta_{3j+1} &= \bar{\theta}, \\ t_{3j+2} - t_{3j+1} &= (1 - 2\alpha)(t_{3j+3} - t_{3j}) & \theta_{3j+2} &= 1 - \bar{\theta}, \\ t_{3j+3} - t_{3j+2} &= \alpha(t_{3j+3} - t_{3j}) & \theta_{3j+3} &= \bar{\theta}. \end{aligned}$$

Hence, three subsequent intervals must form a macro-patch with a regular structure of θ and mesh-size parameter k_j .

Further, let $J: \mathcal{X} \rightarrow \mathbb{R}$ be the error functional and $\text{TOL} > 0$ be the desired tolerance to be reached $|J(\mathbf{u}) - J(\mathbf{u}_k^\theta)| < \text{TOL}$. The adaptive algorithm is based on the iteration of the following steps:

Step 1: Primal solution

On $\{t_m \mid m = 0, 1, \dots, M\}$ approximate the incompressible Navier–Stokes equations with the theta or fractional step theta method (compare Problem 2) for $m = 1, 2, \dots, M$ and given $\mathbf{v}_{k,0}^\theta := \mathbf{v}^0$:

$$\begin{aligned} (\mathbf{v}_{k,m}^\theta - \mathbf{v}_{k,m-1}^\theta, \boldsymbol{\varphi}) + \theta k_m a(\mathbf{v}_{k,m}^\theta, \boldsymbol{\varphi}) + (1 - \theta) k_m a(\mathbf{v}_{k,m-1}^\theta, \boldsymbol{\varphi}) - k_m b(p_{k,m}^\theta, \boldsymbol{\varphi}) + k_m b(\xi, \mathbf{v}_{k,m}^\theta) \\ = \theta k_m (\mathbf{f}(t_m), \boldsymbol{\varphi}) + (1 - \theta) k_m (\mathbf{f}(t_{m-1}), \boldsymbol{\varphi}) \quad \forall (\boldsymbol{\varphi}, \xi) \in \mathbf{V} \times H. \end{aligned}$$

Step 2: Adjoint solution

On $\{t_m \mid m = 0, 1, \dots, M\}$, given the discrete solution of Step 1, solve for the adjoint solution backward in time. Here, we need to adapt the first and the last step, see Section 3.2:

• Step M:

$$\begin{aligned} (\bar{\mathbf{w}}_{k,M}^\theta, \boldsymbol{\varphi}) + \theta_M k_M a'(\mathbf{v}_{k,M}^\theta)(\boldsymbol{\varphi}, \bar{\mathbf{w}}_{k,M}^\theta) + k_M b(q_{k,M}^\theta, \boldsymbol{\varphi}) - k_M b(\xi, \bar{\mathbf{w}}_{k,M}^\theta) \\ = J'(\mathbf{v}_{k,M}^\theta, p_{k,M}^\theta)(\boldsymbol{\varphi}, \xi) \quad \forall (\boldsymbol{\varphi}, \xi) \in \mathbf{V} \times H. \end{aligned}$$

• Steps $M - 1, M - 2, \dots, 1$:

$$\begin{aligned} -(\bar{\mathbf{w}}_{k,m+1}^\theta - \bar{\mathbf{w}}_{k,m}^\theta, \boldsymbol{\varphi}) + \theta_m k_m a'(\mathbf{v}_{k,m}^\theta)(\boldsymbol{\varphi}, \bar{\mathbf{w}}_{k,m}^\theta) + (1 - \theta_{m+1}) k_{m+1} a'(\mathbf{v}_{k,m}^\theta)(\boldsymbol{\varphi}, \bar{\mathbf{w}}_{k,m+1}^\theta) \\ + k_m b(q_{k,m}^\theta, \boldsymbol{\varphi}) - k_m b(\xi, \bar{\mathbf{w}}_{k,m}^\theta) \\ = J'(\mathbf{v}_{k,m}^\theta, p_{k,m}^\theta)(\boldsymbol{\varphi}, \xi) \quad \forall (\boldsymbol{\varphi}, \xi) \in \mathbf{V} \times H. \end{aligned}$$

• Step 0:

$$-(\bar{\mathbf{w}}_{k,1}^\theta - \bar{\mathbf{w}}_{k,0}^\theta, \boldsymbol{\varphi}) + (1 - \theta_1) k_1 a'(\mathbf{v}_{k,0}^\theta)(\boldsymbol{\varphi}, \bar{\mathbf{w}}_{k,1}^\theta) = 0 \quad \forall \boldsymbol{\varphi} \in \mathbf{V}.$$

Step 3: Error estimation

On $\{t_m \mid m = 0, 1, \dots, M\}$, given the solution of primal $\mathbf{u}_k = (\mathbf{v}_k^\theta, p_k^\theta)$ and adjoint $\mathbf{z}_k = (\mathbf{w}^\theta, q_k^\theta)$ problem, calculate the fluctuations $\mathbf{u}_k^{(2)} - \mathbf{u}_k$ and $\mathbf{z}_k^{(2)} - \mathbf{z}_k$ accordingly to Section 3.3. Next, evaluate the error estimator on every

time-interval I_m :

$$\eta_m := \rho(\mathbf{u}_k)(z_k)|_{I_m} + \frac{1}{2} \left\{ \rho(\mathbf{u}_k)(z_k^{(2)} - z_k)|_{I_m} + \rho^*(\mathbf{u}_k, z_k)(\mathbf{u}_k^{(2)} - \mathbf{u}_k)|_{I_m} \right\}.$$

This is the error estimator from [Theorem 1](#). However, the residuals are restricted to the interval $I_m = (t_{m-1}, t_m]$ only. For evaluation of these residuals, it is necessary to use a higher order numerical quadrature rule, like the two-point Gauss rule. Next, we check, if the desired error tolerance has been reached:

$$\left| \sum_{m=1}^M \eta_m \right| < \text{TOL}.$$

If this is the case, we stop the algorithm and the numerical approximation \mathbf{u}_k is the solution.

Step 4: Time mesh adaptation

If the error tolerance has not been reached, we use the information of η_m to construct a new temporal mesh. Here, we need to distinguish between the theta and the fractional step theta method. We first describe the case of the simple theta method.

Time mesh adaptation is based on subdividing intervals I_m , if the absolute value of the corresponding error indicator $|\eta_m|$ is larger than the average. This is a simple error averaging technique. Hence, we first compute the average

$$\bar{\eta} = \frac{1}{M} \sum_{m=1}^M |\eta_m|$$

and subdivide I_m into two intervals by introducing

$$t_{m-\frac{1}{2}} := \frac{t_{m-1} + t_m}{2}$$

if the error indicator is above average:

$$|\eta_m| > \sigma^{(1)} \bar{\eta} \implies \text{split } (t_{m-1}, t_m] \text{ into } (t_{m-1}, t_{m-\frac{1}{2}}] \text{ and } (t_{m-\frac{1}{2}}, t_m].$$

Further, we combine two time intervals I_m and I_{m+1} , if the summed error is smaller than the desired threshold:

$$|\eta^m| + |\eta^{m+1}| \leq \sigma^{(2)} \frac{\text{TOL}}{M} \implies \text{combine } (t_{m-1}, t_m] \text{ and } (t_m, t_{m+1}] \text{ to } (t_{m-1}, t_{m+1}].$$

By $\sigma^{(1)} \approx 1$ and $\sigma^{(2)} < 1$ we denote constants, that control the sharpness of refinement.

In the case of the fractional step theta method, we first agglomerate the error indicators to the macro intervals:

$$\eta_j^{FST} = \eta_{3j} + \eta_{3j+1} + \eta_{3j+2}, \quad I_j^{FST} = I_{3j} \cup I_{3j+1} \cup I_{3j+2}, \quad j = 1, 2, \dots, \frac{M}{3}.$$

The adaptation process is then carried out on I_j^{FS} using η_j^{FST} . After adaptation of the macro mesh, we reintroduce the substeps.

5. Numerical examples

As numerical test-cases, we consider variants of the benchmark problem ‘‘laminar flow around a cylinder’’ introduced by Turek and Schäfer [9]. This benchmark was introduced to establish well-defined test cases for different numerical approaches to computational fluid dynamics. Here, we slightly adapt the setting such that the temporal discretization gets more significant.

[Fig. 2](#) shows the geometric configuration of this benchmark problem. As in the original description, we set the density to $\rho = 1$ and the kinematic viscosity to $\nu = 10^{-3}$. The inflow profile on Γ^{in} is parabolic in x_2 -direction and depends on the time as

$$\mathbf{v}^{\text{in}}(x, t) = \frac{3}{2} \bar{\mathbf{v}}^{\text{in}}(t) \mathbf{v}^{\text{in}}(x) \quad \text{with } \mathbf{v}^{\text{in}}(x) = \frac{4x_2(H - x_2)}{H^2},$$

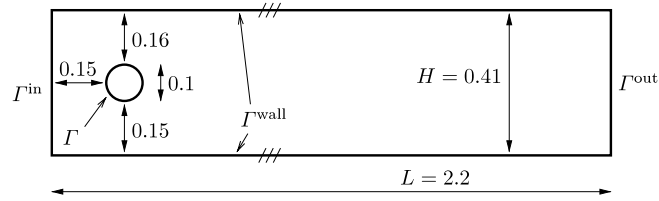


Fig. 2. Configuration of the benchmark problem.

where $H = 0.41$ denotes the height of the channel. The average inflow velocity $\bar{v}^{\text{in}}(t)$ will be specified for each of the two test-cases.

5.1. Spatial discretization

This paper deals with the temporal discretization only. Hence, we will run all simulations on fixed spatial meshes with approximately $N \approx 10\,000$ degrees of freedom. For the space discretization, we choose a stabilized equal-order finite element pair with piece-wise bi-quadratic velocities and pressures. For stabilization of the inf–sup condition, we use the Local Projection Stabilization method (LPS) by Becker and Braack [10] based on a projection into the inf–sup stable Taylor–Hood element pair. The spatial discretization is sufficiently fine, such that stabilization of convective terms is not necessary for this low Reynolds number problem. The resulting nonlinear algebraic problems are solved with a Newton iteration. All linear systems are approximated using a geometric multigrid solver.

5.2. Test case 1: Measuring the error at final time

In this first test-case, we choose a smooth profile for the average inflow velocity in the time-interval $I = (0, 3)$ as $\bar{v}^{\text{in}}(t) = t$. With a maximum average inflow velocity of $\bar{v}^{\text{max}} = 3$, this configuration gives Reynolds numbers in the range $0 \leq \text{Re} \leq 300$. We choose as functional the squared “vorticity” of the solution at final time $T = 3$ given by

$$J_{\text{vort}}(\mathbf{u}) = j_{\text{vort}}(\mathbf{u}(T)) := \int_{\Omega} |\partial_2 v_1(T) - \partial_1 v_2(T)|^2 dx.$$

In Fig. 3 we show the vorticity as function of the complete time-interval. With increasing inflow velocity, the vorticity increases with time, and for large velocities, the solution features some oscillations that are also visible in the functional. For comparison, we compute a reference value on very fine temporal meshes with up to $M = 327\,680$ time-steps using a globally stable shifted variant of the Crank–Nicolson scheme, see [11]. With help of extrapolation, we identify the reference value

$$\bar{J}_{\text{vort}} = 2702.1 \pm 0.1,$$

which relates to a relative error of about $\pm 0.05\%$.

We run computations with the fractional step theta scheme using $\theta = 0.55$ and we initially choose 30 uniform macro time-steps with step size $k = 0.1$. The error estimator is approximated as described in the previous sections. For higher order approximation of \mathbf{u}_k^θ and \mathbf{z}_k^θ , we choose a quadratic interpolation between two adjacent macro-time steps, e.g. t_m, t_{m+1}, t_{m+2} and we neglect all intermediate solutions $t_{m \pm \alpha}$.

In Table 1 we show the number of macro time-steps N , the value of the functional $J(\mathbf{u}_k^\theta)_{\text{vort}}$, the temporal discretization error $|\bar{J}_{\text{vort}} - J(\mathbf{u}_k^\theta)_{\text{vort}}|$, the estimator value η split into quadrature error η^G , primal η^P and adjoint η^D residual and finally the effectivity index given by the quotient of estimator by error on a sequence of locally refined meshes.

We get good effectivities on all temporal meshes with values close to one starting from 1000 macro-steps. Using small time step sizes, the Galerkin error is dominant. Here, we point out, that the Galerkin formulation is only considered as trick for error estimation, this formulation does not limit the accuracy of the discrete approximation. Adaptive mesh refinement does not yield any substantial benefit, as the temporal regularity of this test case is very high. Measuring the functional error at final time $T = 3$ calls for an uniform refinement of the complete time-interval.

5.3. Test case 2: Adaptive time-step control

In this second test-case we consider a different inflow profile, similar to the original benchmark-setting from Turek & Schäfer [9]. Here however, we pick a temporal inflow profile with lower regularity: The average velocity of the

Table 1

Test case 1. Number of macro time-steps, functional value (final vorticity), error, total estimator, split into Galerkin part, primal, dual residuals and finally the effectivity as quotient between estimator value and real error. Computations done on uniform temporal meshes.

N	J	Error	η	η^G	η^P	η^D	Eff
30	3006.21	304.11	150.59	-28.92	126.162	53.348	0.50
60	2779.26	77.16	126.25	13.18	74.223	38.848	1.63
120	2731.05	28.95	9.95	18.49	-4.760	-3.778	0.34
240	2716.32	14.22	26.50	14.73	7.739	4.031	1.86
480	2711.09	8.99	12.55	8.98	2.178	1.393	1.40
960	2706.91	4.81	5.89	4.99	0.553	0.342	1.22
1920	2704.55	2.45	2.89	2.66	0.144	0.087	1.18
3840	2703.34	1.24	1.43	1.37	0.039	0.024	1.15
7680	2702.72	0.62	0.72	0.70	0.011	0.008	1.16
15360	2702.42	0.32	0.36	0.35	0.004	0.003	1.13

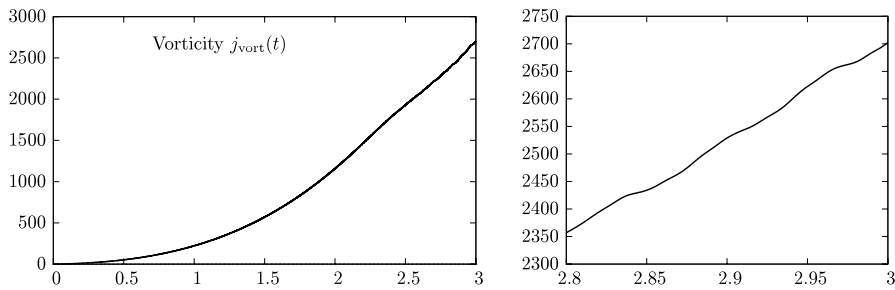


Fig. 3. The vorticity as function over the time-interval $I = [0, 3]$ and a zoom around the final time.

parabolic inflow profile raises linearly from zero to one in $I_1 = [0, 2]$, stays constant in $I_2 = [2, 6]$ and falls back to zero in $I_3 = [6, 8]$:

$$\bar{v}^{\text{in}}(t) = \begin{cases} \frac{t}{2}, & t \in [0, 2), \\ 1, & t \in [2, 6], \\ 4 - \frac{t}{2}, & t \in (6, 8]. \end{cases}$$

Here, we consider as functional the mean value of the lift in the sub-interval (5, 6):

$$J_{\text{lift}}(\mathbf{u}) := \int_5^6 j_{\text{lift}}(\mathbf{u}(t)) dt = \int_5^6 \int_{\Gamma} \mathbf{n} \cdot (\nabla \mathbf{v}(t) - p(t)\mathbf{I}) \mathbf{e}_2 do dt.$$

In Fig. 4, we show the lift as function over the complete time-interval. The lift is very sensitive with respect to temporal and spatial resolution. The results shown in the figure refers to a computation on a fine mesh with more than 1000 time steps. A reference value is identified by computations on very fine temporal meshes (more than 10^6 time steps) and using extrapolation:

$$\bar{J}_{\text{lift}} = -0.02337 \pm 10^{-5}.$$

This reference value carries a relative error of about $\pm 0.05\%$.

Adaptive time-mesh control is carried out as described in Step 4 of the adaptive algorithm described in the previous section. In Fig. 5, we show the slopes of the relative errors on uniform and locally refined temporal grids as well as the value of the error estimator for the adaptive refinement procedure. By using adaptive mesh refinement, an error of 1% in the functional can be reached on meshes with 10 times less time-steps. Further, we show the splitting of the estimator into quadrature error and primal and dual residuals. Again, the influence of the quadrature error decreases on fine meshes.

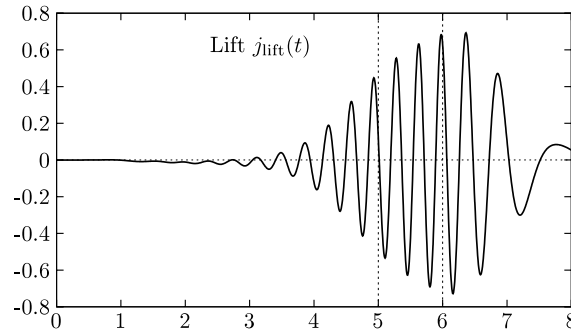


Fig. 4. Test case 2. The functional (lift) plotted over the time-interval. Here, we measure the average of the lift over the sub-interval (5, 6).

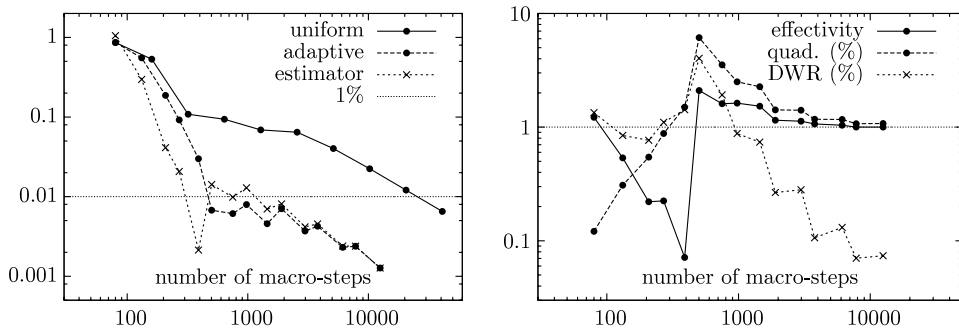


Fig. 5. Test case 2. Left: comparison between uniform and adaptive meshes. Right: effectivity of the error estimator and division of the estimator into quadrature error and DWR error.

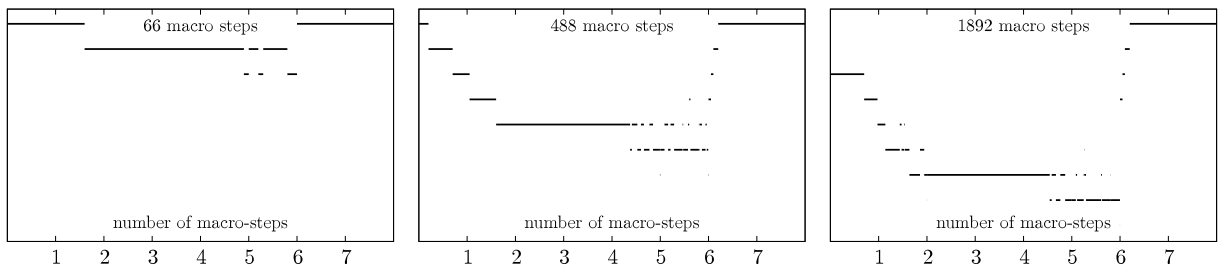


Fig. 6. Test case 2. Locally adapted time-meshes with 66, 488 and 1892 macro time steps.

In Fig. 6, we finally show three different time meshes. Obviously, no refinement is necessary for all times $t > 6$, as the adjoint solution z is zero here. Further, the a posteriori error estimator shows a focus on the evaluation interval (5, 6).

6. Conclusion and outlook

In this contribution, it has been shown, that the dual weighted residual method can be used for time error estimation and time mesh control for the incompressible Navier–Stokes equations discretized with the fractional step theta method. As this time-stepping scheme is based on a difference approximation, for error estimation a Galerkin scheme similar to it is considered and the error estimator is split into a quadrature error and a Galerkin defect.

It remains to combine this technique with spatial mesh adaptivity using dynamic as discussed in [12]. Where the high effort of dynamic mesh control is not adequate, spatial mesh adaptivity can be based on averaged error quantities are discussed by Braack et al. [13].

References

- [1] M.O. Bristeau, R. Glowinski, J. Periaux, Numerical methods for the Navier–Stokes equations, *Comput. Phys. Rep.* 6 (1987) 73–187.
- [2] S. Turek, L. Rivkind, J. Hron, R. Glowinski, Numerical study of a modified time-stepping theta-scheme for incompressible flow simulations, *J. Sci. Comput.* 28 (2–3) (2006) 533–547.
- [3] D. Meidner, T. Richter, Goal oriented error estimation for the fractional step theta time stepping scheme, *Comput. Methods Appl. Math.* (2014) ahead of print.
- [4] R. Becker, R. Rannacher, Weighted a posteriori error control in FE methods, in: H.G. Bock (Ed.), *ENUMATH 1997*, World Sci. Publ, Singapore, 1995.
- [5] R. Becker, R. Rannacher, An optimal control approach to a posteriori error estimation in finite element methods, in: A. Iserles (Ed.), in: *Acta Numerica*, 37, Cambridge University Press, 2001, pp. 1–225.
- [6] M. Besier, R. Rannacher, Goal-oriented space–time adaptivity in the finite element Galerkin method for the computation of nonstationary incompressible flow, *Internat. J. Numer. Methods Fluids* 70 (2012) 1139–1166.
- [7] C. Goll, R. Rannacher, W. Wollner, The damped Crank–Nicolson time-marching scheme for the adaptive solution of the Black–Scholes equation, *J. Comp. Finance* (2014) in press.
- [8] D. Meidner, B. Vexler, A priori error analysis of the petrov-galerkin crank-nicolson scheme for parabolic optimal control problems, *SIAM J. Control Optim.* 49 (5) (2011) 2183–2211.
- [9] M. Schäfer, S. Turek, Benchmark computations of laminar flow around a cylinder. (With support by F. Durst, E. Krause and R. Rannacher), in: E.H. Hirschel (Ed.), *Flow Simulation with High-Performance Computers II. DFG Priority Research Program Results 1993–1995*, in: *Notes Numer. Fluid Mech.*, 52, Vieweg, Wiesbaden, 1996, pp. 547–566.
- [10] R. Becker, M. Braack, A finite element pressure gradient stabilization for the stokes equations based on local projections, *Calcolo* 38 (4) (2001) 173–199.
- [11] J. Heywood, R. Rannacher, Finite element approximation of the nonstationary Navier–Stokes problem. IV, Error analysis for second-order time discretization, 27 (3) (1990) 353–384.
- [12] M. Schmich, B. Vexler, Adaptivity with dynamic meshes for space–time finite element discretizations of parabolic equations, *SIAM J. Sci. Comput.* 30 (1) (2008) 369–393.
- [13] M. Braack, E. Burman, N. Taschenberger, Duality based a posteriori error estimation for quasi periodic solutions using time averages, *SIAM J. Sci. Comput.* 33 (2011) 2199–2216.